



Utrecht University

On modelling the Earth

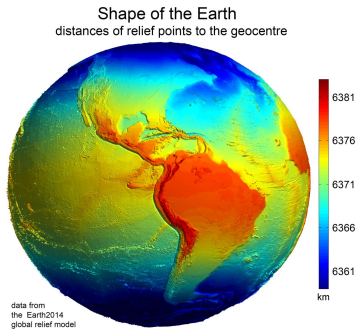
c.thieulot@uu.nl



$\sim 4.54 \cdot 10^9$ years old

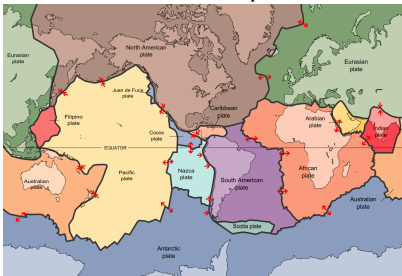
$\sim 6 \cdot 10^{24}$ kg

The Earth (1)

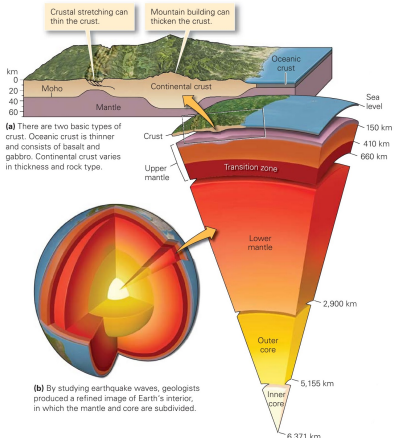


$$\delta R/R \simeq 0.3\%$$

Plate tectonics theory:



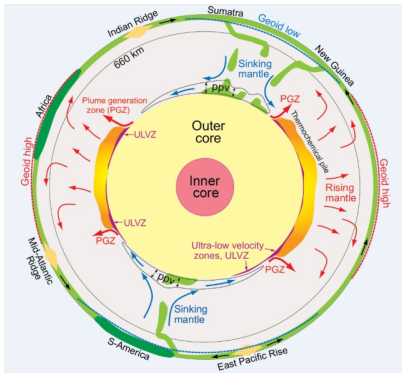
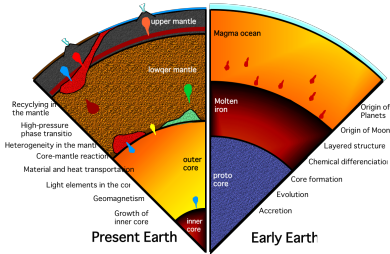
The Earth (2)



The solid earth interacts with:

- the hydrosphere
- the atmosphere
- the biosphere

The Earth (3)



[Trønnes, Mineral. Petrol., 2010]

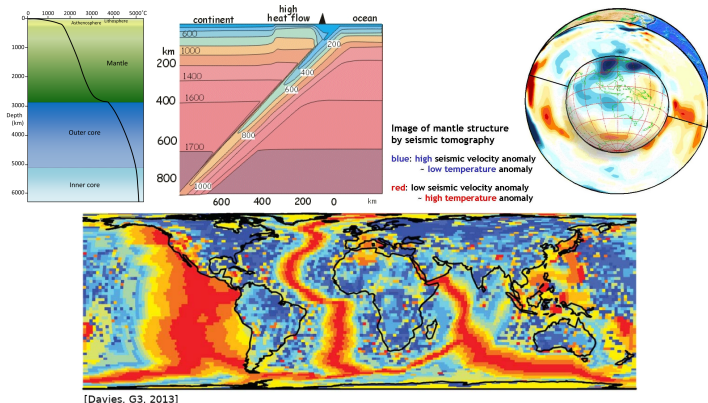
The Earth (4)

- Complex dynamical system → I will focus on the Solid Earth.
- Maxwell relaxation time: $t_M = \eta/\mu \simeq 10^3$ yr. Elastic behaviour can be neglected when studying phenomena taking place at Myr scale (e.g. mantle convection) but not for short phenomena (e.g. Earthquakes, glacial rebound).
- Reynold's number $Re = \rho u L / \eta \sim 10^{-20}$ → inertia negligible

"It is no exaggeration to say that the theory of slow viscous flow is the very heart of geodynamics." Neil Ribe, 2018.

The Earth (5)

Earth is a heat engine: internal heat is a combination of residual heat from planetary accretion ($\sim 20\%$) and radioactive decay ($\sim 80\%$).



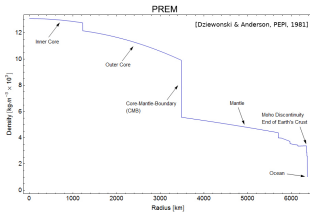
Final Estimate of Heat Flow (mW m^{-2}) (Area-weighted Mean)

The Earth (6)



I need to solve the
mass, momentum, energy
conservation equations for Stokes flow
+
additional (geo)physics ?

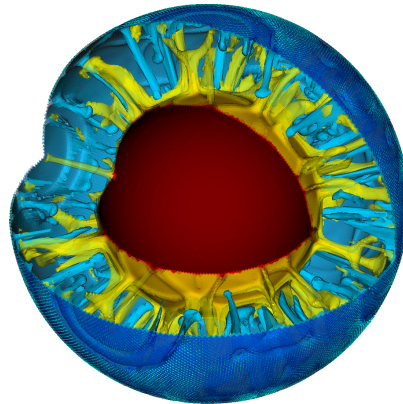
The Earth (7)



- Outer Core viscosity $\sim 1 \text{ Pa.s}$ but mantle viscosity $\eta_m > 10^{21} \text{ Pa.s}$
→ core dynamics inaccessible to solid Earth modellers.
- simple:** Earth is a giant Rayleigh-Bénard experiment in a perfectly spherical hollow sphere with

$$Ra = \frac{\rho_0^2 \alpha \Delta T D^3 g C_p}{\eta k} \sim 10^6 - 10^8 >> Ra_c$$

The Earth (7)



1200 cores, 24h wall time, 70 Mdofs, 1000 time steps.

<https://youtu.be/j63MkEc0RRw>

The Earth (7)



Wait a second ... ?

Rheology (1)

What is the rheology of the fluid(s)?

What are the mantle and the crust made of?

- mantle is 45% O, 22% Si, and 23% Mg (+ Fe, Al, Ca, Na, K)
- These elements are all bound together in the form of silicate rocks (e.g. olivine, pyroxenes, spinel, and garnet).
- These rocks are subjected to large ΔT (10^3 K) and ΔP (10^9 Pa).
- Long time scales: viscous flow
- They have undergone 4Byr of deformation (mix? anisotropy?)
- They contain water (or not? how much? where?)
- The mineral grain size changes

Rheology (1)



Phenocrysts in ultramafic picritic rock, 5cm



Olivine with pyrope and chromian diopside in peridotite, 25cm



Basalt or picrite with olivine 6cm



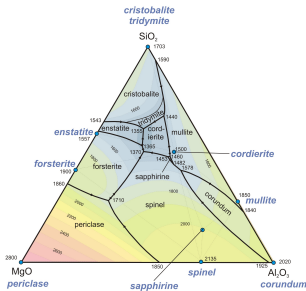
Dunite with dark green chlorite, 11cm

Rheology (2)

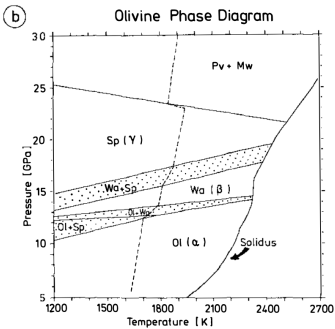
Welcome to the fun world of geochemistry/petrology!

The three-component chemical system $\text{MgO}-\text{Al}_2\text{O}_3-\text{SiO}_2$

(MAS) accounts for 89% of the Earth's mantle.



The system $\text{MgO}-\text{Al}_2\text{O}_3-\text{SiO}_2$ at 1 atm. pressure



[Christensen, Annu. Rev. Earth Planet Sci. 1995]

Rheology (3) - ductile regime

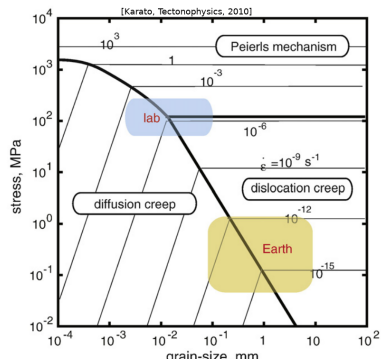
Lab experiments



Triaxial compression apparatus (Utrecht Univ.)

confining press. up to 100 MPa, temp. up to 400^o C,

constant strain rate (10^{-4} - 10^{-7} s⁻¹).



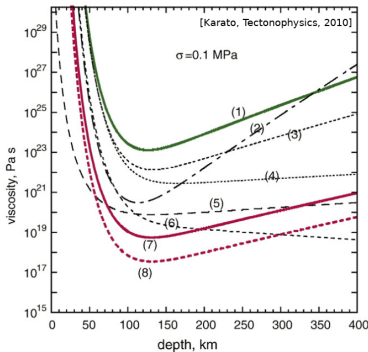
(valid for P=7GPa, T=1700K)

$$\dot{\epsilon} = A \left(\frac{\sigma}{\mu} \right)^n \left(\frac{b}{d} \right)^m \exp \left(- \frac{Q + pV}{RT} \right)$$

[Karato & Wu, Science, 1993]

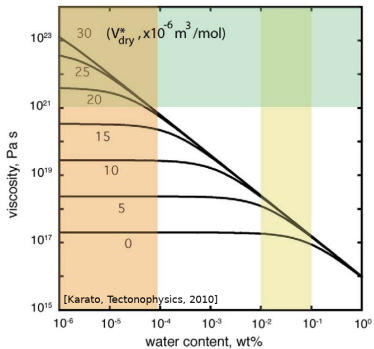
Rheology (3) - ductile regime

Different labs:



upper mantle with a typical oceanic geotherm calculated
from the power-law creep const. relationship for olivine

Water content



The influence of water depletion on viscosity (at 200 km
depth: $P = 7$ GPa, $T = 1700$ K, $\sigma = 0.1$ MPa)

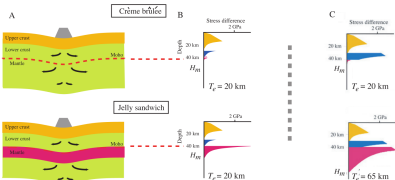
Rheology (4) - brittle regime

When stress reaches the yield value, the rock breaks:



The long-term strength of continental lithosphere: “jelly sandwich” or “crème brûlée”?

E.B. Burov, Laboratoire de Tectonique, University of Paris 6,
4 Place Jussieu, 75252 Paris Cedex 05, France, evgenii.burov@
lgs.jussieu.fr, and **A.B. Watts**, Department of Earth Sciences,
University of Oxford, Parks Road, Oxford OX1 3PR, UK, tony.
watts@earth.ox.ac.uk



Viscous-plastic rheologies (yield criterion)
faults = high deformation rate zones of narrow width.

[Duretz et al, G3, 2018; Spiegelman et al, G3, 2016; Thieulot et al, in prep.]

Rheology (5) - Putting it all together



Available online at www.sciencedirect.com

ScienceDirect

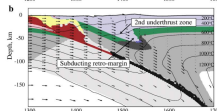
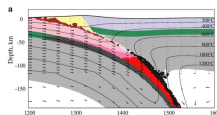
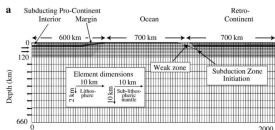
Earth and Planetary Science Letters 267 (2008) 129–140

EPSL

www.elsevier.com/locate/epsl

Modelling tectonic styles and ultra-high pressure (UHP) rock exhumation during the transition from oceanic subduction to continental collision

C.J. Warren^{a,*}, C. Beaumont^b, R.A. Jamison^a



Parameters used in models

Mechanical parameters (reference)	Units	Pro-interior upper/mid crust	Pro-margin upper/mid crust	Retro-upper/ mid crust	Lower crust	Oceanic crust	Continental mantle lithosphere	Oceanic mantle lithosphere	Sub-lithospheric mantle
Thickness	km	24	24(max)	24	12	8	84	82	To 660 km depth
Ref density	kg m ⁻³	2800	2800	2800	2950	2900	3250	3250	3250
Ref density T	K	473	473	473	773	273	1609	1609	1609
Density HP	kg m ⁻³	2800–2900	2800–2900	2800–2900	3100	3300			
Density UHP	kg m ⁻³	2800–3000	2800–3000	2800–3000					
ϕ_{at}	deg	15–2	15–2	15–2	15–2	15–2	15–2	15–2	15–2
Cohesion	MPa	20	20	20	0	0	0	0	0
Flow law		Wet	Wet	Dry Maryland	Dry Maryland	Wet	Wet	Wet	Wet Olivine
		Quartzite	Quartzite	Quartzite	Diabase	Diabase	Olivine	Olivine	
Reference		Gleason and Tullis (1995)	Gleason and Tullis (1995)	Gleason and Tullis (1995)	Mackwell	Mackwell	Karato and Karato and	Karato and Karato and	
							Wu (1993)	Wu (1993)	
<i>F</i>		5	5	5	0.1	0.1	10	10	1
<i>N</i>		4	4	4	4.7	4.7	3	3	3
<i>B*</i> ^a	Pa s ^{1/4}	2.92 × 10 ⁸	2.92 × 10 ⁶	2.92 × 10 ⁶	1.91 × 10 ⁵	1.91 × 10 ⁵	1.92 × 10 ⁴	1.92 × 10 ⁴	1.92 × 10 ⁴
<i>Q</i>	kJ mol ⁻¹	223	223	223	485	485	430	430	430
<i>P*</i>	m ³ mol ⁻¹	0	0	0	0	0	1.0 × 10 ⁻⁵	1.0 × 10 ⁻⁵	1.0 × 10 ⁻⁵
<i>S1: Continental subduction</i>									
Heat capacity	m ² K s ⁻²	750	750	750	750	750	1250	1250	1250
Thermal conductivity	W m ⁻¹ K ⁻¹	2.25	2.25	2.25	2.25	2.25	2.25	2.25	52
Thermal diffusivity	m ² s ⁻¹	1.0 × 10 ⁻⁶	1.0 × 10 ⁻⁶	1.0 × 10 ⁻⁶	1.0 × 10 ⁻⁶	0.6 × 10 ⁻⁶	0.6 × 10 ⁻⁶	1.4 × 10 ⁻⁶	1.4 × 10 ⁻⁵
Thermal expansion	K ⁻¹	3.0 × 10 ⁻⁵	3.0 × 10 ⁻⁵	3.0 × 10 ⁻⁵	3.0 × 10 ⁻⁵	3.0 × 10 ⁻⁵	3.0 × 10 ⁻⁵	3.0 × 10 ⁻⁵	3.0 × 10 ⁻⁵
Heat production	μW m ⁻³	1.15	1.15	1.15	0.75	0	0	0	0
<i>Reference Model Set 1</i>									
Cold-weak									
<i>f</i>		5	1	5	0.1	0.1	10	10	1
Heat production	μW m ⁻³	1.15	1.15	1.15	0.75	0	0	0	0
Hot-strong									
<i>f</i>		5	5	5	0.1	0.1	10	10	1
Heat production	μW m ⁻³	1.15	2.0	1.15	0.75	0	0	0	0
Hot-weak									
<i>f</i>		5	1	5	0.1	0.1	10	10	1
Heat production	μW m ⁻³	1.15	2.0	1.15	0.75	0	0	0	0
$\Delta\rho = -10$ kg m ⁻³ Density	kg m ⁻³	2800	2800	2800	2950	2900	3240	3240	3250
$\Delta\rho = +10$ kg m ⁻³ Density	kg m ⁻³	2800	2800	2800	2950	2900	3260	3260	3250
$\Delta\rho = +20$ kg m ⁻³ Density	kg m ⁻³	2800	2800	2800	2950	2900	3270	3270	3250

Rheology (5) - Putting it all together



Available online at www.sciencedirect.com

ScienceDirect

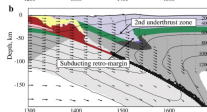
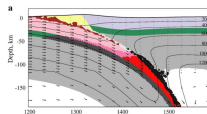
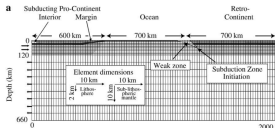
Earth and Planetary Science Letters 267 (2008) 129–140

EPSL

www.elsevier.com/locate/epsl

Modelling tectonic styles and ultra-high pressure (UHP) rock exhumation during the transition from oceanic subduction to continental collision

C.J. Warren^{a,*}, C. Beaumont^b, R.A. Jamison^a



Parameters used in models

Mechanical parameters (reference)	Units	Pro-interior upper/mid crust	Pro-margin upper/mid crust	Retro-upper/ mid crust	Lower crust	Oceanic crust	Continental mantle lithosphere	Oceanic mantle lithosphere	Sub-lithospheric mantle
Thickness	km	24	24(max)	24	12	8	84	82	To 660 km depth
Ref density	kg m ⁻³	2800	2800	2800	2950	2900	3250	3250	3250
Ref density T	K	473	473	473	773	273	1609	1609	1609
Density HP	kg m ⁻³	2800–2900	2800–2900	2800–2900	3100	3300			
Density UHP	kg m ⁻³	2800–3000	2800–3000	2800–3000					
ϕ_{sat}	deg	15–2	15–2	15–2	15–2	15–2	15–2	15–2	15–2
Cohesion	MPa	20	20	20	0	0	0	0	0
Flow law		Wet	Wet	Wet	Dry Maryland	Wet	Wet	Wet	Wet Olivine
		Quartzite	Quartzite	Quartzite	Diabase	Diabase	Olivine	Olivine	
Reference		Gleason and Tullis (1995)	Gleason and Tullis (1995)	Gleason and Tullis (1995)	Mackwell et al. (1998)	Mackwell et al. (1998)	Karato and Wu (1993)	Karato and Wu (1993)	Karato and Wu (1993)
F		5	5	5	0.1	0.1	10	10	1
N		4	4	4	4.7	4.7	3	3	3
B^*	$\text{Pa s}^{1/4}$	2.92×10^8	2.92×10^6	2.92×10^6	1.91×10^5	1.91×10^5	1.92×10^4	1.92×10^4	1.92×10^4
Q	kJ mol^{-1}	223	223	223	485	485	430	430	430
I^*	$\text{m}^3 \text{mol}^{-1}$	0	0	0	0	0	1.0×10^{-5}	1.0×10^{-5}	1.0×10^{-5}
S1: Continental subduction									
Heat capacity	$\text{m}^2 \text{K s}^{-2}$	750	750	750	750	750	1250	1250	1250
Thermal conductivity	$\text{W m}^{-1} \text{K}^{-1}$	2.25	2.25	2.25	2.25	2.25	2.25	2.25	52
Thermal diffusivity	$\text{m}^2 \text{s}^{-1}$	1.0×10^{-6}	1.0×10^{-6}	1.0×10^{-6}	1.0×10^{-6}	0.6×10^{-6}	0.6×10^{-6}	1.4×10^{-6}	1.4×10^{-5}
Thermal expansion	K^{-1}	3.0×10^{-5}	3.0×10^{-5}	3.0×10^{-5}	3.0×10^{-5}	3.0×10^{-5}	3.0×10^{-5}	3.0×10^{-5}	3.0×10^{-5}
Heat production	$\mu\text{W m}^{-3}$	1.15	1.15	1.15	0.75	0	0	0	0
Reference Model Set 1									
Cold-weak									
f		5	1	5	0.1	0.1	10	10	1
Heat production	$\mu\text{W m}^{-3}$	1.15	1.15	1.15	0.75	0	0	0	0
Hot-strong									
f		5	5	5	0.1	0.1	10	10	1
Heat production	$\mu\text{W m}^{-3}$	1.15	2.0	1.15	0.75	0	0	0	0
Hot-weak									
f		5	1	5	0.1	0.1	10	10	1
Heat production	$\mu\text{W m}^{-3}$	1.15	2.0	1.15	0.75	0	0	0	0
$\Delta\rho = -10 \text{ kg m}^{-3}$ Density	kg m^{-3}	2800	2800	2800	2950	2900	3240	3240	3250
$\Delta\rho = +10 \text{ kg m}^{-3}$ Density	kg m^{-3}	2800	2800	2800	2950	2900	3260	3260	3250
$\Delta\rho = +20 \text{ kg m}^{-3}$ Density	kg m^{-3}	2800	2800	2800	2950	2900	3270	3270	3250

Rheology (5) - Putting it all together

A flow law for dislocation creep of quartz aggregates determined with the molten salt cell

Gayle C. Gleason ^{*1}, Jan Tullis

Department of Geological Sciences, Brown University, Providence, RI 02912, USA

Received 11 May 1994; accepted 25 January 1995

Abstract

We have used the molten salt cell to conduct an experimental study on the rheology of a natural quartzite containing ~ 0.15 wt. % water. Co-axial deformation experiments were conducted at constant piston displacement rates, approximating constant strain rates at low strain. The strengths of our natural quartzite measured in the molten salt cell are approximately half those measured at the same conditions in solid media because, unlike solid confining media, molten salt does not contribute to the strength of the sample; it reduces the friction on the moving piston, and it allows clear identification of the 'hit' point. We have limited the experimental conditions to those required for dislocation creep, and have used only steady-state flow stresses measured during climb-accommodated dislocation creep to calculate the flow law parameters. Two flow laws were determined, one for samples containing minor amounts of melt (1–2%) and one for melt-free samples. In both cases, the power law stress exponent, n , is 4.0 ± 0.9 , which is greater than that previously reported in flow laws for dislocation creep of quartz aggregates determined in solid media. The activation energy, Q , is 137 ± 34 kJ mol $^{-1}$ for samples with melt and 223 ± 56 kJ mol $^{-1}$ for those without, within the range of previously determined values for quartz aggregates containing ~ 0.1 wt.% water. The pre-exponential term, A , is $1.1 \times 10^{(-4.4 \pm 2)}$ MPa $^{-n}$ s $^{-1}$ for samples without melt and $1.8 \times 10^{(-8.1 \pm 2)}$ MPa $^{-n}$ s $^{-1}$ for those with melt. The lower strengths measured in the molten salt cell indicate that previous piezometer relations for quartz experimentally determined in solid media are not correct. Extrapolation of the flow law for melt-free aggregates to natural strain rates predicts higher strengths than most previous quartz flow laws. However, accurate extrapolation requires determining the dependence of flow stress on $f_{\text{H}_2\text{O}}$ and/or a_{H^+} .

$$\dot{\varepsilon} = A \left(\frac{\sigma}{\mu} \right)^n \left(\frac{b}{d} \right)^m \exp \left(-\frac{Q + pV}{RT} \right)$$

Analogue modelling (1)

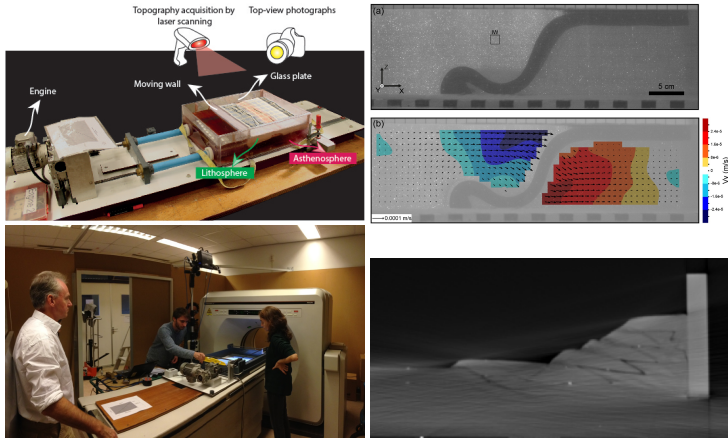


(Cadell, 1888)

Materials for analogue modelling^[1]

Categories	Examples	Simulation
Granular materials (various in density, shape, and size)	Quartz sand, glass microbeads, feldspar powder	Brittle upper crust ^[8]
Low-viscous materials	Water, sugar solution, honey	Asthenosphere,
	Corn syrup, glucose syrup	Sub-lithospheric mantle
High linear viscous materials	Syrup, silicone putty	Sinking slabs ^[23]
Visco-elastic materials	Amorphous polymers, biopolymers, bitumen	Ductile lithosphere
Non-linear viscous materials	Plastic materials	Plasticine
	Visco-plastic materials	Wax, paraffin
	Visco-elasto-plastic materials	Gelatin

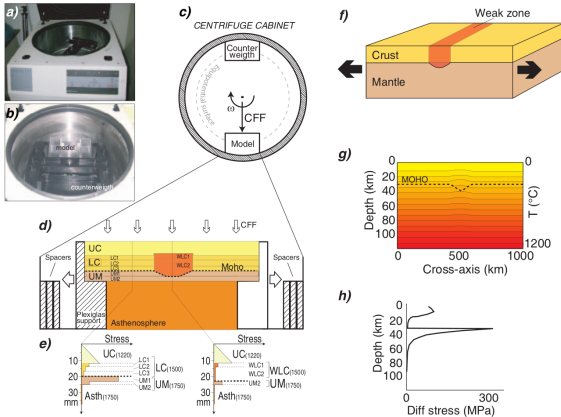
Analogue modelling (2)



[Koyi, Journal of Petroleum Geology, 1997; Graveleau et al, Tectonophysics, 2012; Schellart & Strak, J. of Geodyn., 2016]

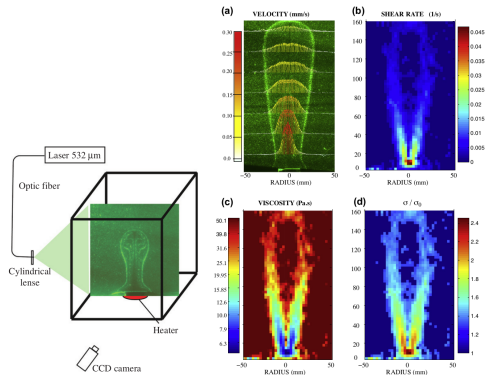
Analogue modelling (3)

'easy' to change density & viscosity, geometries, but gravity?



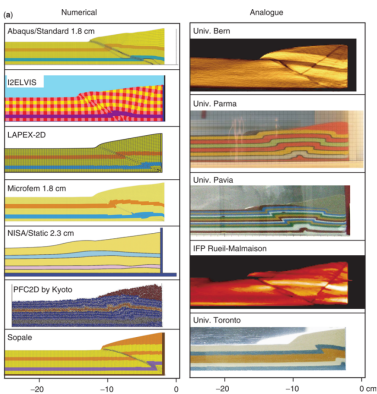
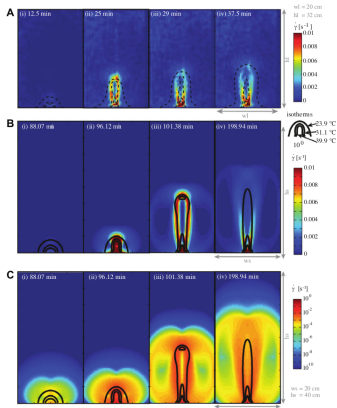
[Corti, Nature Geo, 2008]

Analogue modelling (4)



Herschel-Bulkley fluid (carbopol) is seeded with three types of encapsulated thermo-chromic liquid crystals (TLC), each reflecting light at a different temperature.

Analogue vs Numerical ?



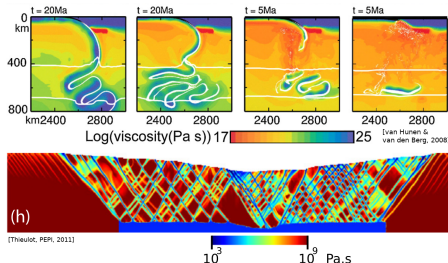
[Massmeyer et al, J. of Non-Newtonian Mech., 2013]

[Buiter et al, Geological Society London, 2006]

Computational geodynamics

What the community needs:

- open-source, well documented & tested code (+ funding)
- flexible physics/numerics
- state-of-the-art numerical methods
- massively parallel
- capable to handle large viscosity contrasts



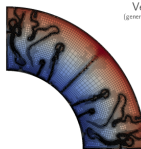
[Thieulot, PEPI, 2011]

Computational geodynamics - ASPECT

COMPUTATIONAL INFRASTRUCTURE FOR GEODYNAMICS (CIG)



Advanced Solver for Problems in Earth's Convection



User Manual

Version 2.2.0-pre

(generated September 2, 2019)

Wolfgang Bangerth
Juliane Dannberg
Rene Gassm  ler
Timo Heister

with contributions by:
Jacqueline Austermann, Magali Billek, Markus Birg, Samuel Cox, William Darkin, Grant Euen,
Menno Frater, Thomas Geffen, Anne Glens, Ryan Grove, Eric Heise, Louise Kellogg, Scott
Kirkpatrick, Michael Klemperer, Michael Knepley, Michael Langford, Michael Lippert, Bob
Myhill, John Nabroff, Bart Nijss, Jonathan Perry-Hoyle, Elbridge Gerry Puckett, Tahiry Pa-
jamanor, Ian Rose, D. Sarah Stamps, Cedric Thieulot, Wanling Wang, Ims van Zelt, Sieg
Zhang

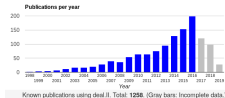
geodynamics.org

<https://github.com/geodynamics/aspect>

<https://geodynamics.org/cig/software/aspect/>

<https://www.dealii.org/>

- developed on deal.II (FE library, 20+ years existence)



- 600+ tests
- 550+ page up-to-date manual (doxygen)
- community (hackathons)



Computational geodynamics - ASPECT features

C++

2D/3D

Compressible & incompressible flow

Cartesian & Spherical geometries

FEM (deal.II) ($Q_2 \times Q_1$ or $Q_2 \times P_{-1}$)

Trilinos (or PETSc) parallel iterative solver

Adaptive mesh refinement AMR (p4est)

Extensively benchmarked

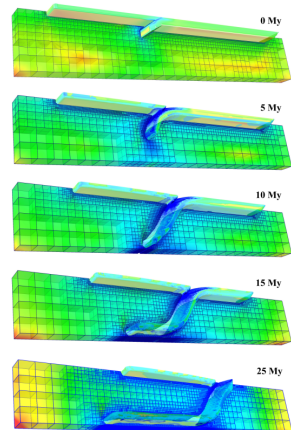
[Kronbichler et al, GJI, 2012; Tosi et al, G3, 2015; Dannberg & Heister, GJI,

2016; Heister et al, GJI, 2017; Thieulot, S.E. 2017; Glerum et al, SE, 2018;

Liu & King, GJI, 2019]

<http://www.p4est.org/>

<https://trilinos.github.io/>



[Glerum et al., Solid Earth, 2018]

Computational geodynamics - Numerical algos.

$$\begin{pmatrix} A & B^T \\ B & 0 \end{pmatrix} \cdot \begin{pmatrix} \boldsymbol{\nu} \\ \boldsymbol{\mathcal{P}} \end{pmatrix} = \begin{pmatrix} \mathbf{f} \\ \mathbf{g} \end{pmatrix}$$

Stokes system → saddle point problem solved with FGMRES.

Right preconditioner

$$P = \begin{pmatrix} \widetilde{A^{-1}} & -\widetilde{A^{-1}B^T}\widetilde{S^{-1}} \\ 0 & \widetilde{S^{-1}} \end{pmatrix}$$

where $\widetilde{A^{-1}}, \widetilde{S^{-1}}$ approximate the exact inverses.

- $\widetilde{A^{-1}}$: CG (loose tol), precond with AMG (and now GMG)
- $\widetilde{S^{-1}}$: inverse of the Schur complement matrix $S = BA^{-1}B^T$ approx. by the inv. of a (weighted) mass matrix in pressure space, precond with ILU.

Computational geodynamics - Numerical algor.

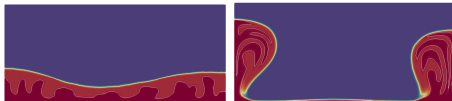
Energy equation (Temperature): advection-diffusion equation with high Peclet number

$$Pe = h|v|/\kappa \sim 10^2 - 10^4$$

- advection is stabilised: Entropy stabilisation [Guermond et al, JCP, 2011] or SUPG [Brooks & Hughes, CMAME, 1982]
- time discretisation: second-order accurate implicit/explicit time stepping scheme based on the BDF-2 scheme [Hairer & Wanner, 1991]
- FE system solved with CG (implicit diff., explicit adv.)

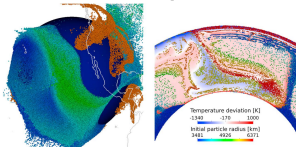
[Kronbichler et al, GJI, 2012]

Computational geodynamics - Material tracking



[Louis-Napoleon et al, in prep.]

- Field based method ("compositions") [Kronbichler, GJI, 2012]
- Discontinuous Galerkin (+BPL) [He et al, PEPI, 2017]
- Volume of Fluid (WIP) [Puckett et al, PEPI, 2018]
- Marker-in-cell [Gassmoeller et al, G3, 2018; GJI, 2019]



also (Particle) Level Set [Bourgouin et al, GJI, 2007; Braun et al, PEPI, 2008; Samuel & Emonuk, G3, 2010]

The Earth (6)



I need to solve the
mass, momentum, energy
conservation equations for Stokes flow
+
additional (geo)physics ?

Computational geodynamics - Melt

Geophysical Journal International

Geophys. J. Int. (2016) 207, 1343–1366
 Advance Access publication 2016 September 4
 GfG Geodynamics and tectonics

doi:10.1093/gji/ggv729



Compressible magma/mantle dynamics: 3-D, adaptive simulations in ASPECT

Juliane Dannberg^{1,2,*} and Timo Heister³

The melt fraction ϕ defines averaged quantities \bar{x} out of solid (X_s) and fluid (X_f) quantities:

$$\bar{x} = (1 - \phi)X_s + \phi X_f, \quad (1)$$

We start from the McKenzie equations, which are derived in appendix A of McKenzie (1984). The mass and momentum conservation for solid and fluid are:

$$\frac{\partial}{\partial t} [\rho_s \phi] + \nabla \cdot [\rho_s \phi \mathbf{u}_s] = \Gamma, \quad (2)$$

$$\frac{\partial}{\partial t} [\rho_f (1 - \phi)] + \nabla \cdot [\rho_f (1 - \phi) \mathbf{u}_f] = -\Gamma, \quad (3)$$

$$\phi (\mathbf{u}_s - \mathbf{u}_f) = -K_0 (\nabla p_f - \rho g), \quad (4)$$

$$-\nabla \cdot [2u_s \left(u_s - \frac{1}{3}(\nabla \cdot \mathbf{u}_s) \mathbf{I} \right) + \frac{2}{3}(\nabla \cdot \mathbf{u}_s) \mathbf{I}] + \nabla p_f = \eta \mathbf{g}, \quad (5)$$

where ρ is the density (with the index denoting solid or fluid phase), \mathbf{g} is the gravitational acceleration, Γ is the melting rate, and the other symbols are as given in Table 1. In order to eliminate the time derivatives, and under the assumption that the flow field is in equilibrium ($\partial p_s / \partial t = 0$), we rewrite the first two equations to:

$$\frac{\partial \phi}{\partial t} + \nabla \cdot [\phi \mathbf{u}_s] = \frac{\Gamma}{\rho_f} - \frac{\partial}{\partial t} \frac{\phi}{\rho_s} \mathbf{u}_s \cdot \nabla p_f, \quad (6)$$

$$-\frac{\partial \phi}{\partial t} + \nabla \cdot [(1 - \phi) \mathbf{u}_f] = \frac{\Gamma}{\rho_s} - \frac{1 - \phi}{\rho_f} \mathbf{u}_f \cdot \nabla p_f. \quad (7)$$

Now we can add eqs (6) and (7) and get

$$\nabla \cdot [\phi \mathbf{u}_s + (1 - \phi) \mathbf{u}_f] = \Gamma \left(\frac{1}{\rho_f} - \frac{1}{\rho_s} \right) \quad (8)$$

$$-\frac{\partial \phi}{\partial t} \mathbf{u}_f \cdot \nabla p_f - \frac{1 - \phi}{\rho_s} \mathbf{u}_f \cdot \nabla p_f.$$

To eliminate the fluid velocity \mathbf{u}_f from the equations, we replace it by using Darcy's law (eq. 4):

and get

$$\begin{aligned} \nabla \cdot \mathbf{u}_s - \nabla \cdot [K_0 (\nabla p_f - \rho g) \mathbf{u}_s] \\ = \Gamma \left(\frac{1}{\rho_f} - \frac{1}{\rho_s} \right) - \frac{\phi}{\rho_s} \mathbf{u}_s \cdot \nabla p_f + \frac{K_0}{\rho_s} (\nabla p_f - \rho g) \cdot \nabla p_f \\ - \frac{1 - \phi}{\rho_s} \mathbf{u}_s \cdot \nabla p_f. \end{aligned} \quad (10)$$

Rearranging terms, we get

$$\begin{aligned} \nabla \cdot \mathbf{u}_s - \nabla \cdot [K_0 (\nabla p_f - \rho g) \mathbf{u}_s] - \frac{\nabla p_f}{\rho_s} \\ = -\nabla \cdot [K_0 (\phi \mathbf{u}_s^2) \mathbf{I}] + \Gamma \left(\frac{1}{\rho_f} - \frac{1}{\rho_s} \right) \\ - \frac{\phi}{\rho_s} \mathbf{u}_s \cdot \nabla p_f - \frac{1 - \phi}{\rho_s} \mathbf{u}_s \cdot \nabla p_f - K_0 \mathbf{g} \cdot \nabla p_f \quad \text{in } \Omega. \end{aligned} \quad (11)$$

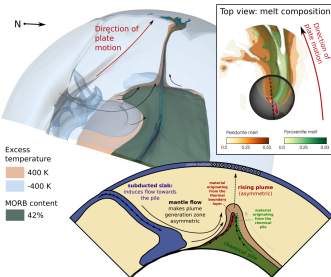
The last three terms contain gradients of the solid and fluid density, respectively, and are typically nonlinear. As densities are typically model specific input parameters, modelling of these terms has to be considered. The change in density of the solid phase is dominated by the change in static pressure, which can be written as $\nabla p_s \approx \nabla p_{\text{true}} \approx \rho_s \mathbf{g}$. This allows us to write

$$\frac{1}{\rho_s} \nabla p_s \approx \frac{1}{\rho_s} \frac{\partial \rho_s}{\partial p} \nabla p_f \approx \frac{1}{\rho_s} \frac{\partial \rho_s}{\partial p} V p_{\text{true}} \approx \frac{1}{\rho_s} \frac{\partial \rho_s}{\partial p} \rho_s \mathbf{g} = \kappa_s \mathbf{g} \cdot \mathbf{g}, \quad (12)$$

where κ_s is the isothermal compressibility of the solid. To approximate the fluid density using the fluid pressure gradient, the chosen model parameters have to be considered. If viscous compaction is large compared to Darcy drag, the fluid pressure is controlled by the melt density. On the other hand, if viscous compaction is small compared to Darcy drag, the fluid pressure is controlled by the solid density. Solid and melt density can also be expressed in terms of the compaction length $\delta_c = \sqrt{(\Gamma + 4\eta/3)K_0}$, with a small δ_c compared to size of the melting region corresponding to the latter, and a large δ_c corresponding to the former case. Hence, we make $V p_f$ a model input parameter, which can be adapted based on which

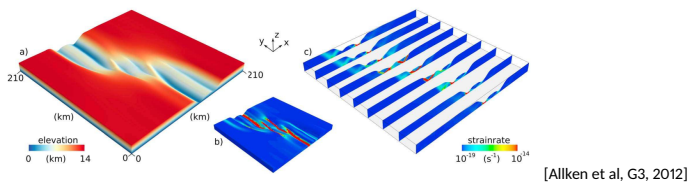
Chemical trends in ocean islands explained by plume–slab interaction

Juliane Dannberg^{1,2,*} and René Gassmöller^{1,3,†}



[Gerya & Meilick, JMG, 2011; Keller et al, GJI, 2013; Bouilhol et al, EPSL, 2005; Baes et al, EPSL, 2016; ...]

Computational geodynamics - free surface



- Arbitrary Lagrangian Eulerian formulation (FEM codes)
[Fullsack, GJI, 1995; Thieulot, PEPI, 2011, Rose et al, PEPI, 2017]
- Sticky-air approach (FDM, FVM, FEM). Air layer has to (a) be sufficiently thick and (b) have sufficiently low viscosity
 $\eta_{air} = 10^{17} - 10^{19} \text{ Pa.s}$ [Quinquis et al, Tectonophysics, 2011; Cramer et al, GJI, 2012]
Sometimes supplemented with Marker-and-chain.

Computational geodynamics - More!

- Grain-size evolution

Geochemistry, Geophysics, Geosystems

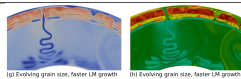
RESEARCH ARTICLE

10.1002/2017GC006944

Key Points:
• A new, implemented dynamically
evolving grain size into whole-mantle

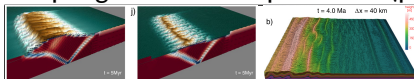
The importance of grain size to mantle dynamics and
seismological observations

J. Dandekar^{1,2} ● Z. Elion^{1,3} ● Ulrich Faul¹ ● René Gassmoller^{1,2} ● Pritviraj Moulik⁴ ● and
Robert Myhill¹ ●



[Solomatov, EPSL, 2001; Cerpa et al, JGR, 2017]

- Coupling with surface processes (paleo-climate)



[Braun & Yamato, Tect., 2010; Braun & Willett, Geomorph., 2013; Thieulot et al, G3, 2014; Ueda et al, Tect., 2015]

- PDEs are highly nonlinear: tailored Newton solver



- Seismo-thermo-poro-elasto-visco-plastic modelling

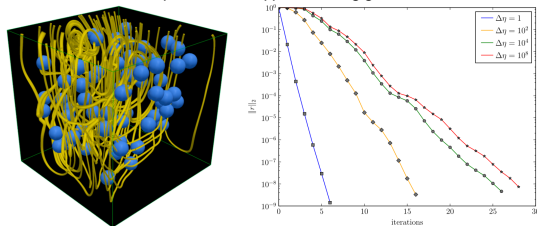
[van Dinther et al, GRL, 2014; Gerya, 2018]

Computational geodynamics - FEM + PETSc

A scalable, matrix-free multigrid preconditioner for finite element discretizations of heterogeneous Stokes flow

D.A. May^{a,*}, J. Brown^{b,c,d}, L. Le Pourhiet^{e,f}

Comput. Methods Appl. Mech. Engrg., 2015

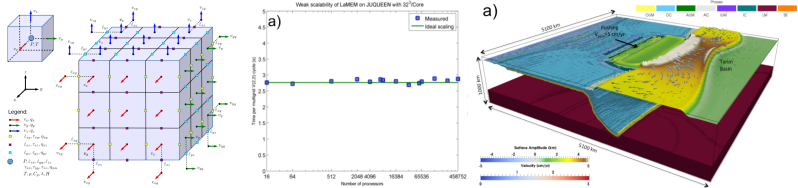


Matrix-free operators reduce storage and memory bandwidth requirements → improved speed and scalability on modern multi-core hardware.

Computational geodynamics - FDM + PETSc

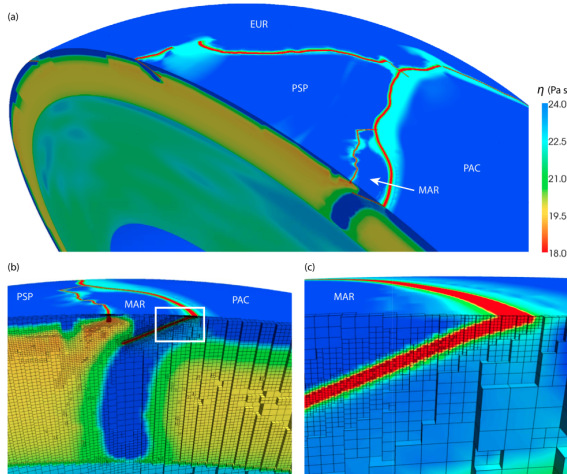
Forward and Inverse Modelling of Lithospheric Deformation on Geological Timescales

Boris J. P. Kaus^{1,2,3}, Anton A. Popov¹, Tobias S. Baumann¹, Adina E. Püsök¹, Arthur Bauville¹, Naiara Fernandez^{1,4}, and Marine Collignon⁵



[Collignon et al, G3, 2014; Tectonophysics, 2015; Fernandez & Kaus, GJI, 2015; Pusok et al, 2018]

Computational geodynamics - FEM



200-300 million elements, 400-1200 Mdofs, 4000-5000 procs
+ inverse techniques [Stadler et al, Science, 2010; Alisic et al, JGR, 2012]

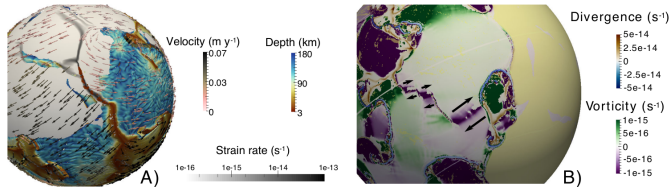
Computational geodynamics - FVM

What drives tectonic plates?

Nicolas Coltice^{1*}, Laurent Husson², Claudio Faccenna^{3,4}, Maëlis Arnould¹

Science Advances, in press, 2019

One sentence summary: Numerical models handling both lithosphere and mantle convection as a single self-organizing system show the dynamic balance between plates and mantle shifts over a supercontinent cycle.



1.5 Byr, 50M cells, wall time: 9 months, 128 cores, 390k time steps.

Conclusions

- Earth is fascinating object, but very complex
- Analogue & numerical modelling
- Computational geodynamics benefits from state-of-the-art CFD
- Multi-physics: *extremely* nonlinear coupled PDEs (strategy?)
- Physical length-scale vs mesh resolution
- Initial geometry and temperature field remain a problem
- Reproducibility?

Geodynamical Modelling =



or

